Quantum plasmons in double layer systems

Luis Brey[1] and H. A. Fertig[1,2,3]

[1]*Instituto de Ciencia de Materiales de Madrid (CSIC), Cantoblanco, 28049 Madrid, Spain*
[2]*Quantum Science and Engineering Center, Indiana University, Bloomington, Indiana 47408, USA*
[3]*Department of Physics, Indiana University, Bloomington, Indiana 47405, USA*

Plasmons are fundamental excitations of metals which can be described in terms of electron dynamics, or in terms of the electromagnetic fields associated with them. In this work we develop a quantum description of plasmons in a double layer structure, treating them as confined electromagnetic modes of the structure. The structure of the resulting bosonic Hamiltonian indicates the presence of virtual plasmons of the individual layers which appear as quantum fluctuations in the ground state. For momenta smaller than the inverse separation between layers, these modes are in the ultrastrong coupling regime. Coherence terms in the Hamiltonian indicate that modes with equal and opposite momenta are entangled. We consider how in principle these entangled modes might be accessed, by analyzing a situation in which the conductivity of one of the two layers suddenly drops to zero. The resulting density matrix has a large entanglement entropy at small momenta, and modes at $\pm\mathbf{q}$ that are inseparable. More practical routes to releasing and detecting entangled plasmons from this system are considered.

I. INTRODUCTION

In metals, Coulomb interactions among carriers yield self-sustained collective charge density oscillations, which, when quantized, are called plasmons [1–5]. In three dimensions, because of the long-range nature of the interaction, the plasmon spectrum is gapped, and in the long wavelength limit its energy is given by $\hbar\Omega$, where Ω is the classical plasma frequency. Two-dimensional (2D) realizations of plasmons can also be found at the surface of a metal [6] or in 2D conducting materials [7–10]. In these systems the plasmon spectrum is gapless, vanishing as $\sim\sqrt{q}$, where q is the 2D momentum. An interesting distinction between three- and two-dimensional plasmons is that in the latter, the electric field associated with the density oscillations exists outside the material, allowing strong coupling to other electromagnetic sources and modes. Indeed, in such systems the collective modes may be described completely in terms of electromagnetic degrees of freedom, so that the plasmons may be understood as confined light modes and are known as surface-plasmon-polaritons [11–14].

Among systems that support 2D plasmons, graphene has emerged as a particularly remarkable platform. Graphene is a single layer of carbon atoms arranged in a honeycomb network; in pristine form it is a semimetal, but it can easily be made metallic using the electric field effect [15,16]. It is an interesting material in the context of plasmons because it is open to the environment, allowing their direct visualization in near-field microscopy experiments [17–19]. Moreover, graphene may be patterned or gated to create plasmonic metamaterials [20], and is particularly attractive for photonics and nanooptoelectronics [17,21,22] because it supports long propagation lengths [23], and can be tuned such that the relevant frequencies are in the terahertz range.

As with light, many interesting and useful physical phenomena associated with plasmons in graphene can be understood in a purely classical framework [17–20,24–33]. However, as in optics [34,35], the underlying quantum structure of the plasmons allows for behaviors that are purely quantum mechanical in nature. For example, a quantum treatment of surface plasmons is necessary for modeling stimulated emission of quantum emitters [36], quantum correlations between plasmons [37–39], or coupling effects mediated by plasmons [40–42].

In this work we investigate the quantum properties of plasmons in a double layer (DL) graphene system, as illustrated in Fig. 1(a). The layers, labeled T (top) and B (bottom), are separated by an insulator barrier thick enough to prevent electron tunneling, but thin enough for the interlayer Coulomb interaction to be important [43–45]. The qualitative behavior of collective plasmon modes in such double layer systems has been well-known for some time [46], in particular that they support in-phase optical modes and out-of-phase acoustic modes [see Fig. 1(b)]. We demonstrate that in a quantum description, the ground state contains a finite number of virtual plasmons in the T and B layers, as illustrated in Fig. 1(c). Energy conservation dictates that these virtual excitations cannot be withdrawn from the system directly [37]; however, in the presence of time dependence in the Hamiltonian, their presence can have highly nontrivial consequences. We consider a protocol in which the electron density in one layer is dropped suddenly to zero. Because of the presence of the virtual plasmons, plasmons that emerge in the remaining charged layer have strong quantum correlations. In particular, we find a large entanglement entropy among these plasmons. Moreover, we show that the density matrices for plasmons with momenta $\pm\mathbf{q}$ are generically inseparable [47,48] so that correlations between these two modes are intrinsically quantum
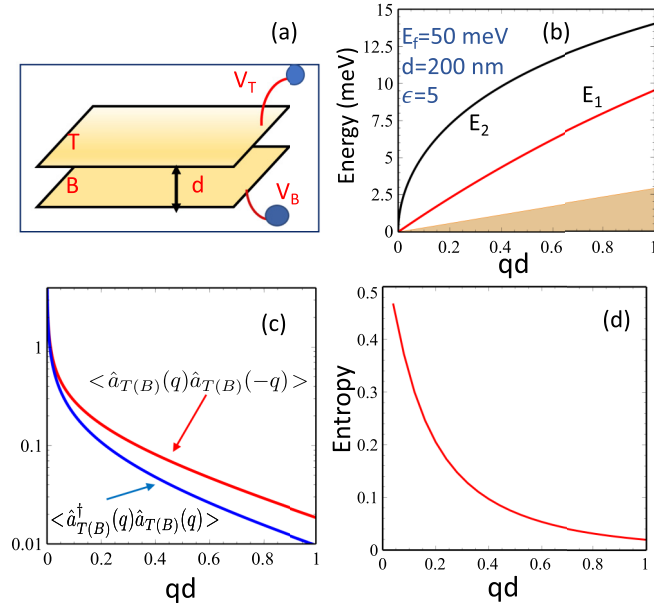
045303-1

FIG. 1. (a) Scheme of the DL system. (b) Dispersion of the acoustic, E_2, and optical plasmons, E_1, of a DL for the parameters indicated in the figure. The plasmons do not overlap with the electron-hole continuum, shadow region, indicating they have a long lifetime. (c) Population and intralayer coherence of virtual plasmons in T or B layers as function of qd. (d) Entropy associated with the entanglement of plasmons in T and B layers.

in nature, i.e., they cannot be explained within any classical description.

Our proposal to generate correlated plasmons from vacuum quantum fluctuations of the double layer system by temporal perturbation of the Hamiltonian has similarities with studies of time-varying systems in which electromagnetic vacuum fluctuations can result in the generation of real photons [49,50]. These dynamical vacuum effects are generically known as dynamical Casimir effects, and have been studied extensively for their potential applications as quantum light sources. For example, there are proposals for the excitation of quantum radiation and photon generation by temporal modulation of the dielectric constant of a medium [51,52]. Photons can also be generated from a cavity with an effective time-dependent mirror [53]. Moreover, in monolayer graphene, the generation of plasmon pairs from vacuum fluctuations by a periodic modulation of the substrate permittivity has been proposed [54,55].

II. PRELIMINARIES: 2D PLASMONS AS CONFINED ELECTROMAGNETIC MODES

In what follows we model 2D metals as dissipationless conductors, characterized by an optical conductivity that, for small momenta and frequencies, takes the form [56–58] $\sigma(\omega; E_F) = i\frac{D}{\omega}$, where $D = \frac{e^2 E_F}{\hbar^2 \pi}$ is the Drude weight and E_F is the Fermi energy. In graphene, E_F is related to the density of carriers, n_0, through the relation $E_F = \hbar v_D \sqrt{\pi n_0}$, with v_D the velocity of the graphene Dirac points [8,15,16]. Semiclassically, in 2D the plasmon frequency, $\omega_q = \sqrt{\frac{D}{2\epsilon_d \epsilon_0}q}$ (with ϵ_d is

the dielectric constant of the surrounding medium), and the corresponding electric and magnetic fields can be obtained from Maxwell's equations, with proper matching of the fields across the 2D metal sheet, taking into account the optical conductivity $\sigma(\omega; E_F)$ [11,59].

We proceed to write a quantum Hamiltonian for the electromagnetic field associated with plasmons, making some simplifying assumptions. Specifically we assume the semistatic limit, which is appropriate when the plasmons wavelength is much smaller than the light wavelength at the same frequency. In this situation the magnetic field contribution to the electromagnetic energy is negligible (see the SM). Our Hamiltonian then becomes [59–64]

$$
\begin{aligned}
\hat{H} &= \frac{\epsilon_0 \epsilon_d}{2} \iint d\mathbf{r}\,dz\,\hat{\mathbf{E}}(\mathbf{r}, z)\hat{\mathbf{E}}(\mathbf{r}, z) \\
&+ \frac{1}{2} \iint d\mathbf{r}\,dz\,D\delta(z)\hat{\mathbf{A}}(\mathbf{r}, z)\hat{\mathbf{A}}(\mathbf{r}, z) \\
&= \sum_{\mathbf{q}} \frac{\hbar\omega_q}{2}(\hat{a}_{\mathbf{q}}\hat{a}_{\mathbf{q}}^\dagger + \hat{a}_{\mathbf{q}}^\dagger \hat{a}_{\mathbf{q}}),
\end{aligned}
\tag{1}
$$

where the operator $\hat{a}_{\mathbf{q}}$ annihilates a plasmon with 2D momentum $\mathbf{q}$ and frequency ω_q. In terms of $\hat{a}_{\mathbf{q}}$, $\hat{a}_{\mathbf{q}}^\dagger$ the electric field and vector potential operators associated with plasmons have the form

$$
\hat{\mathbf{E}}(\mathbf{r}, z) = \sqrt{\frac{\hbar\omega_q}{2\epsilon_0\epsilon_d S}}e^{i\mathbf{q}\mathbf{r}}\mathbf{u}(\mathbf{q}, z)\hat{a}_{\mathbf{q}} + \text{H.c.},
$$

$$
\hat{\mathbf{A}}(\mathbf{r}, z) = -i\sqrt{\frac{\hbar}{2\epsilon_0\epsilon_d S\omega_q}}e^{i\mathbf{q}\mathbf{r}}\mathbf{u}(\mathbf{q}, z)\hat{a}_{\mathbf{q}} + \text{H.c.},
\tag{2}
$$

where S is the sample area and the vectors $\mathbf{u}(\mathbf{q}, z)$ are given by

$$
\mathbf{u}(\mathbf{q}, z) = e^{-q|z|}\sqrt{\frac{q}{2}}\left(i\frac{\mathbf{q}}{q} - \frac{z}{|z|}\hat{\mathbf{z}}\right).
\tag{3}
$$

In Eq. (1) the first term is the energy stored in the electric field energy and the second term, which is nonzero only in the conducting layer, represents the kinetic energy of the charge carriers.

III. PLASMONS IN DOUBLE LAYER SYSTEM

Consider two metallic sheets, T and B, located at $z = \frac{d}{2}$ and $z = -\frac{d}{2}$, respectively. The separation d is assumed large enough that electron tunneling between the layers can be neglected. The layers are connected to metallic contacts that define their Fermi energies, as illustrated in Fig. 1(a). We assume both layers have the same density of carriers and so the same plasmon dispersion ω_q when isolated.

In the double layer system, the total electric field is the sum of fields generated by the plasmons in the T and B layers. The total electric field operator becomes $\hat{\mathbf{E}}(\mathbf{r}, z) = \hat{\mathbf{E}}^T(\mathbf{r}, z) + \hat{\mathbf{E}}^B(\mathbf{r}, z)$, with

$$
\hat{\mathbf{E}}^{T(B)}(\mathbf{r}, z) = \sum_{\mathbf{q}} \sqrt{\frac{\hbar\omega_q}{2\epsilon_0\epsilon_d S}}e^{i\mathbf{q}\mathbf{r}}\mathbf{u}\left(\mathbf{q}, z \mp \frac{d}{2}\right)\hat{a}_{\mathbf{q}}^{T(B)} + \text{H.c.},
\tag{4}
$$

where $\hat{a}_{\mathbf{q}}^{T(B)}$ annihilates a plasmon with momentum $\mathbf{q}$ in the T(B) layer. Coupling between plasmons in the T and B layers appears in the cross term of the electric field energy, $\hat{V} = \epsilon_0 \epsilon \int d\mathbf{r} dz \, \hat{\mathbf{E}}^T(\mathbf{r}, z) \hat{\mathbf{E}}^B(\mathbf{r}, z)$. By performing the integral of this contribution, the DL Hamiltonian becomes

$$\hat{H} = \hat{H}_T + \hat{H}_B + \hat{V} \qquad (5)$$

with

$$\hat{H}_{T(B)} = \sum_{\mathbf{q}} \hbar\omega_q \left(\hat{a}_{\mathbf{q}}^{T(B)\dagger} \hat{a}_{\mathbf{q}}^{T(B)} + \frac{1}{2} \right)$$

and

$$\hat{V} = \sum_{\mathbf{q}} \frac{\hbar\omega_q}{2} e^{-qd} \left(\hat{a}_{\mathbf{q}}^{T\dagger} \hat{a}_{\mathbf{q}}^{B} + \hat{a}_{\mathbf{q}}^{B\dagger} \hat{a}_{\mathbf{q}}^{T} - \hat{a}_{\mathbf{q}}^{T} \hat{a}_{-\mathbf{q}}^{B} - \hat{a}_{\mathbf{q}}^{B\dagger} \hat{a}_{-\mathbf{q}}^{T\dagger} \right).$$

Equation (5) represents a system of four quantum harmonic oscillators, modes of momentum $\pm\mathbf{q}$ for each of the top and bottom layers, which are all admixed by the interlayer coupling $\hat{V}$. The normal mode frequencies of this coupled system of oscillators can be obtained before quantizing, with the result $\omega_{1(2)}(q) = \omega_q \sqrt{1 \mp e^{-qd}}$. These excitations are the acoustic and optical plasmons of the DL system [46,65]. The present formulation allows one to go beyond a classical treatment to analyze the quantum properties of the coupled plasmon system. The first two terms of the coupling $\hat{V}$ are the resonant part of the interaction, and describe the creation of a plasmon in one layer and the annihilation of a plasmon in the other, while conserving momentum. The last two terms correspond to processes which are nonconserving in the number of plasmons: they simultaneously create or annihilate pairs of plasmons with opposite wave vectors. In quantum optics, such contributions to the Hamiltonian are known as counter-rotating (CR) terms [34–36,66–68]. The coupling coefficient $\Omega_{\mathbf{q}} \equiv \frac{\omega(q)}{2} e^{-qd}$ is the q-dependent Rabi frequency of the DL plasmon system.

In problems involving coupling of matter and light, CR terms are often neglected. This rotating wave approximation (RWA) works well when the coefficients of the CR terms are sufficiently small [34–36,66–68]. (Note that this form of the RWA involves dropping a time-independent term from the Hamiltonian because we are working in the Schrödinger picture. In the Heisenberg picture one may work with equations of motion, in which case the RWA is implemented by dropping rapidly oscillating terms). For the present problem the RWA yields plasmon frequencies $\omega_{RWA}^{1(2)} = \omega(q)(1 \mp \frac{e^{-qd}}{2})$, which is a good approximation to the normal mode frequencies when $qd \gg 1$, but fails significantly when $qd \lesssim 1$. The former can be understood as representing the eigenfrequencies of the DL system to first order in perturbation theory in e^{-qd}. At this level of approximation, self-consistency in the electric fields associated with the plasmons is not fully implemented. The importance of the CR terms at long wavelengths is an indication that this system is in the ultrastrong coupling limit, defined as situations in which the Rabi frequency is not small compared to the uncoupled oscillator frequencies [36,67], in this case $\omega(q)$.

For long wavelength plasmons, it is necessary to diagonalize the Hamiltonian including the CR terms. Because the Hamiltonian is bilinear in the field operators, it can

be diagonalized through a Bogoliubov-Hopfield transformation [37,69]. This involves a symplectic transformation of the T and B creation and annihilation operators, which maintains the bosonic commutation relations of the operators while bringing the Hamiltonian, Eq. (5), into diagonal form (see the SM [59]). Explicitly, with a transformation of the form

$$\begin{aligned}\hat{b}_{1(2)}(q) = \frac{1}{\sqrt{2}} (&\cosh\theta_{1(2)}(\hat{a}^T(\mathbf{q}) \mp \hat{a}^B(\mathbf{q})) \\ &+ \sinh\theta_{1(2)}(\hat{a}^{T\dagger}(-\mathbf{q}) \mp a^{B\dagger}(-\mathbf{q}))),\end{aligned} \qquad (6)$$

where $e^{-2\theta_i} = \omega_i(q)/\omega_q$, the transformed Hamiltonian becomes

$$\hat{H} = \sum_{\mathbf{q},i=1,2} \hbar\omega_i(q) \left(\hat{b}_i^\dagger(\mathbf{q}) \hat{b}_i(\mathbf{q}) + \frac{1}{2} \right). \qquad (7)$$

The frequencies $\omega_i(q)$ are identical to the normal mode frequencies obtained in a classical calculation [59].

IV. VIRTUAL PLASMONS AND ENTANGLEMENT

For finite layer separation the ground state of the system is not the vacuum $|0\rangle$ of the uncoupled DL system, for which $\hat{a}^B(\mathbf{q})|0\rangle = \hat{a}^T(\mathbf{q})|0\rangle = 0$, but rather the vacuum $|G\rangle$ of coupled modes, which satisfies $\hat{b}_1(\mathbf{q})|G\rangle = \hat{b}_2(\mathbf{q})|G\rangle = 0$. Because the $b_i(\mathbf{q})$ annihilation operators are linear combinations of annihilation and creation operators $a^{T,B}(\mathbf{q})$ and $a^{T,B\dagger}(\mathbf{q})$ associated with individual layers, the DL vacuum contains a nonvanishing number of plasmons in the T and B layers with inter and intralayer coherence. Explicitly, inverting Eq. (6) one finds the expectation values

$$\langle \hat{a}^{T(B)\dagger}(\mathbf{q}) \hat{a}^{T(B)}(\mathbf{q}) \rangle = \frac{\sinh^2\theta_2 + \sinh^2\theta_1}{2},$$
$$\langle \hat{a}^{T\dagger}(\mathbf{q}) \hat{a}^B(\mathbf{q}) \rangle = \frac{\sinh^2\theta_2 - \sinh^2\theta_1}{2},$$
$$\langle \hat{a}^T(\mathbf{q}) \hat{a}^T(-\mathbf{q}) \rangle = \frac{\sinh 2\theta_1 + \sinh 2\theta_2}{4}. \qquad (8)$$

In Fig. 1(c) we plot $\langle \hat{a}^{T\dagger}(\mathbf{q}) \hat{a}^T(\mathbf{q}) \rangle$ and $\langle \hat{a}^T(\mathbf{q}) \hat{a}^T(-\mathbf{q}) \rangle$ as functions of qd. These plasmons in the vacuum state are virtual and cannot be extracted from the isolated DL system. Note that these expectation values are nonvanishing because of the presence of CR terms in the Hamiltonian, Eq. (5). Since the Rabi frequency decreases exponentially with qd, the average number and the coherence of single-layer plasmons decreases rapidly with qd. Results in Fig. 1 correspond to $E_F = 50$ meV; qualitatively similar results are obtained for other Fermi energies provided they are in the range of energies for which the electronic properties of graphene are well described by the Dirac equation.

Because the system is translationally invariant, $|G\rangle$ is a state with well-defined, vanishing total in-plane momentum. The presence of intralayer coherence between plasmons of opposite wave vector is then an indication that they are entangled: they must be introduced into the ground state in equal and opposite pairs, as can be seen explicitly in the CR terms of $\hat{H}$. We quantify the degree of entanglement as follows. The Hamiltonian [Eq. (5)] is expanded in the number state basis [59,70,71] $|n_{\mathbf{q}}^T, n_{\mathbf{q}}^B, n_{-\mathbf{q}}^T, n_{-\mathbf{q}}^B\rangle$, where $n_{\mathbf{q}}^\nu$ is the

number of plasmons with momentum $\mathbf{q}$ in layer ν, and then diagonalized to obtain the coefficients $\langle n_{\mathbf{q}}^T, n_{\mathbf{q}}^B, n_{-\mathbf{q}}^T, n_{-\mathbf{q}}^B | G \rangle$. These are the probability amplitudes which encode different numbers of single layer plasmons in the ground state. We then compute the reduced density matrix for the subsystem of plasmons in layer T with momentum $\mathbf{q}$,

$$
\rho^{(\mathbf{q})}(n_{\mathbf{q}}^T; n_{\mathbf{q}}^{\prime T})
$$
$$
= \sum_{n_{\mathbf{q}}^B, n_{-\mathbf{q}}^B, n_{-\mathbf{q}}^T} \langle n_{\mathbf{q}}^T, n_{\mathbf{q}}^B, n_{-\mathbf{q}}^T, n_{-\mathbf{q}}^B | \hat{\rho} | n_{\mathbf{q}}^{\prime T}, n_{\mathbf{q}}^B, n_{-\mathbf{q}}^T, n_{-\mathbf{q}}^B \rangle, \quad (9)
$$

where $\hat{\rho}$ is the density operator for the full system. The von Neumann entropy associated with $\rho^{(\mathbf{q})}$ quantifies the entanglement between plasmons of wave vector $\mathbf{q}$ in the top layer and all other plasmon modes (in both the top and bottom layer) [72],

$$
S_{T,\mathbf{q}} = -\sum_i |\lambda_i|^2 \ln |\lambda_i|^2, \quad (10)
$$

where the sum is over the eigenvalues λ_i of the reduced density matrix, $\rho^{(\mathbf{q})}_{n_{\mathbf{q}}^T, n_{\mathbf{q}}^{\prime T}}$. In Fig. 1(d) we plot the entropy $S_{T,\mathbf{q}}$ as a function of the parameter qd. This entropy is nonvanishing because the virtual excitations in the vacuum of the DL involves quantum entanglement among plasmons in the four subsystems ($\pm\mathbf{q}$ for T and B layers.) Again, note that inclusion of the CR terms is crucial to obtaining a nonvanishing entanglement entropy.

V. RELEASING ENTANGLED PLASMONS

The populations of plasmons in the individual layers, which are present in the ground state of the system, are virtual. In order to access them, the quantum Hamiltonian must be perturbed or modulating in some way [37]. One protocol by which this could be done in principle involves a nonadiabatic time-dependent perturbation. In particular, a sudden drop in potential, for example in the bottom layer, can deplete its charge, leaving only the top layer as a remaining host for plasmons. Since in our approach this involves a temporal change in boundary conditions for the electromagnetic field, this is a realization of the dynamical Casimir effect [49,50]. If this switch-off time is shorter than the inverse of a typical Rabi frequency, to a first approximation this represents a sudden change in the Hamiltonian. The loss of mobile charge in the bottom layer eliminates the electric field that it previously generated, so that in Eq. (5), $\hat{H} \to \hat{H}_T$. Although the plasmon degrees of freedom from the bottom layer are formally present in the Hilbert space, they no longer contribute to the dynamics of the system. The initial state of the system after the sudden change is an excited state of $\hat{H}_T$ (in the Hilbert space of both layers), and plasmons which were previously virtual become detectable. Importantly, the intralayer coherence between top layer plasmons with momenta $\mathbf{q}$ and $-\mathbf{q}$, $\langle \hat{a}^T(\mathbf{q}) \hat{a}^T(-\mathbf{q}) \rangle$, indicates they will be entangled. Thus, this geometry in principle offers a source of counter-propagating, entangled plasmons.

In principle, we would like to quantify the degree of entanglement between plasmon modes with equal and opposite momenta. However, the state of these modes by themselves is characterized not by a wave function but rather by a density

matrix, arrived at by tracing out all the other modes from the pure state density matrix. In this situation one evaluates entanglementlike correlations by examining the form of the density matrix. To do this we define the two-mode density matrix,

$$
\rho^{(2)}(n_{\mathbf{q}}^T, n_{-\mathbf{q}}^T; n_{\mathbf{q}}^{\prime T}, n_{-\mathbf{q}}^{\prime T})
$$
$$
= \sum_{n_{\mathbf{q}}^B, n_{-\mathbf{q}}^B} \langle n_{\mathbf{q}}^T, n_{\mathbf{q}}^B, n_{-\mathbf{q}}^B, n_{-\mathbf{q}}^T | \hat{\rho} | n_{\mathbf{q}}^{\prime T}, n_{\mathbf{q}}^B, n_{-\mathbf{q}}^B, n_{-\mathbf{q}}^{\prime T} \rangle. \quad (11)
$$

We would like to know if $\rho^{(2)}$ can be written in the form

$$
\rho^{(2)}(n_{\mathbf{q}}^T, n_{-\mathbf{q}}^T; n_{\mathbf{q}}^{\prime T}, n_{-\mathbf{q}}^{\prime T})
$$
$$
= \sum_i p_i \rho_i^{(\mathbf{q})}(n_{\mathbf{q}}^T; n_{\mathbf{q}}^{\prime T}) \otimes \rho_i^{(-\mathbf{q})}(n_{-\mathbf{q}}^T; n_{-\mathbf{q}}^{\prime T}), \quad (12)
$$

where $0 < p_i < 1$ are real numbers representing probabilities for different states, and $\rho_i^{(\mathbf{q})}$ are single $\mathbf{q}$ mode density matrices for the top layer. If Eq. (12) holds, then $\rho^{(2)}$ represents a mixture of unentangled states. By contrast, if $\rho^{(2)}$ *cannot* be written in this form, the two modes are "inseparable" [48], the generalization of entanglement to a setting where some quantum degrees of freedom have been traced out.

A test of whether Eq. (12) holds was developed in Ref. [47] and is implemented as follows. Writing $\hat{a}_{\pm\mathbf{q}}^T \equiv \frac{1}{\sqrt{2}}(\hat{x}_\pm + i\hat{p}_\pm)$, with $[\hat{x}_s, \hat{p}_{s'}] = i\delta_{s,s'}$, $s, s' = \pm$, one can form EPR-like quadrature operators

$$
\hat{u} = |a|\hat{x}_+ + \frac{1}{a}\hat{x}_-, \quad (13)
$$

$$
\hat{v} = |a|\hat{p}_+ - \frac{1}{a}\hat{p}_-, \quad (14)
$$

where a is a nonvanishing real number. With the definition $\langle \hat{\mathcal{O}} \rangle = Tr[\hat{\rho}^{(2)}\hat{\mathcal{O}}]$, one computes the fluctuations $\langle (\Delta u)^2 \rangle = \langle (\hat{u} - \langle \hat{u} \rangle)^2 \rangle$ and $\langle (\Delta v)^2 \rangle = \langle (\hat{v} - \langle \hat{v} \rangle)^2 \rangle$. If

$$
f(a) \equiv (\langle (\Delta u)^2 \rangle + \langle (\Delta v)^2 \rangle)/(a^2 + 1/a^2) > 1 \quad (15)
$$

for *any* choice of a, the two modes are inseparable.

Figure 2 illustrates the behavior of the fluctuation factor $f(a)$ for different choices of a as a function of qd. One can see clear regions where $f(a) > 1$ for $qd < 1$, particularly for $a \sim -1$ and $a \sim 2$. This demonstrates that plasmon modes $\pm\mathbf{q}$ with $q \lesssim 1/d$ will necessarily have entanglement properties. It should be noted that the criterion in Eq. (15) is a sufficient condition for inseparability, but not a necessary one [47]. Thus, this equation yields a minimal bound on inseparable modes, but modes outside this region may also by inseparable. Nevertheless, the analysis shows unequivocally that some of the plasmon modes generated by the procedure leading to $\rho^{(2)}$ will be inseparable.

The density of emitted plasmons at a given energy immediately after the bottom layer depletion depends on the doping of the DL system and on the layer separation. Figure 3(a) illustrates this for different values of d. For a Fermi energy of 50 meV, dielectric constant $\epsilon_d = 5$, and $d = 10$ nm, the initial population has a maximum near 10 meV and the density of plasmons is of order 10^5 cm^{-2}. This nonmonotonic behavior is present because the density of plasmon states vanishes at zero energy, whereas the population of a given
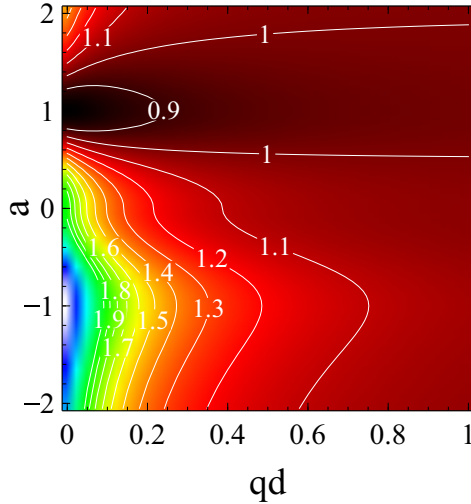
FIG. 2. Fluctuation factor $f(a)$ as function of a and qd (see text). Contour lines indicate level sets of $f(a)$. If $f(a) > 1$ for any a, $\pm \mathbf{q}$ modes at the corresponding qd are inseparable.

mode, $n_{\mathbf{q}} \equiv \langle a_T^{\dagger}(\mathbf{q}) a_T(\mathbf{q}) \rangle$, vanishes at high energy. Because the effective Rabi coupling depends on qd, as the layer separation increases, the maximum moves to smaller wave vectors and so lower energies. The coupling between layers decreases exponentially with d so that the density of virtual plasmons also decreases with increasing d. Interestingly, the density of virtual plasmons in each layer integrated over all momentum depends *only* on d, and is independent of the doping of the layers: $\frac{1}{S} \sum_{\mathbf{q}} n_{\mathbf{q}} \approx \frac{0.0036}{d^2}$.
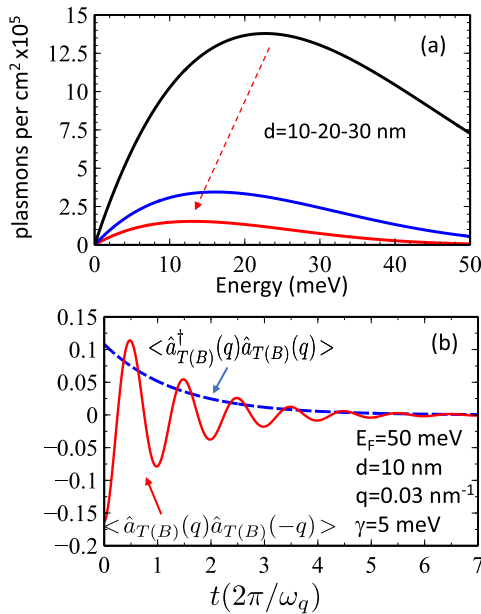

FIG. 3. (a), (b) Number of plasmon per square centimeter as a function of the energy for different values of layer separation d. Time dependence of the number of plasmons and intralayer coherence in the top layer, after the bottom layer is suddenly disconnected. Inset in (b) shows the parameters used in the calculation.

After the bottom layer depletion at time $t = 0$, the time evolution of the density matrix can be modeled using a Markovian master equation, where dissipation in the top layer is introduced perturbatively by means of a Lindblad operator [73],

$$\partial_t \hat{\rho} = -\frac{i}{\hbar}[\hat{H}_T, \hat{\rho}] + \frac{\gamma}{2}\mathcal{L}_{\hat{a}_{\mathbf{q}}^T} + \frac{\gamma}{2}\mathcal{L}_{\hat{a}_{-\mathbf{q}}^T}, \quad (16)$$

where the Lindblad operator associated with a bosonic operator c has the form $\mathcal{L}_c \equiv 2c\hat{\rho}c^{\dagger} - c^{\dagger}c\hat{\rho} - \hat{\rho}c^{\dagger}c$, where $\hat{H}_T$ is the Hamiltonian of the isolated top layer and γ is the (phenomenological) plasmon decay lifetime that, in typical graphene samples, is in the range of meV [17,18,74].

The initial ($t = 0$) form for ρ needed to solve Eq. (16) is the density matrix of the coupled DL plasmon system in the state $|G\rangle$, traced over plasmon states in the bottom layer. Figure 3(b) plots the number of plasmons in the top layer as a function of time as well as the coherence between oppositely propagating plasmons, as obtained from the solution to Eq. (16). The number of plasmons decays exponentially with rate γ, as does the coherence, the latter oscillating with the top layer plasmon frequency ω_q.

VI. SUMMARY AND DISCUSSION

In this paper we have developed the theory of plasmons in a double layer by modeling them as confined electromagnetic modes of the structure, an approach that is particularly appropriate when the electromagnetic coupling between layers is strong. The formalism reproduces the expected dispersion of the plasmon modes, and moreover allows an exploration of their quantum properties. An interesting perspective the approach reveals is the presence of virtual plasmons associated with each layer due to quantum fluctuations. These plasmons are generally entangled, but cannot be released from the ground state without some parametric change in the Hamiltonian. We consider doing this with a form of the dynamical Casimir effect [50,75–78], a sudden depletion of one layer, and find that pairs of plasmons with equal and opposite momenta indeed escape. Immediately after the depletion, plasmons in the $\pm \mathbf{q}$ modes are inseparable for $qd \lesssim 1$, and so will support purely quantum correlations in their populations. Moreover, the modes maintain coherence over a period of time determined by environmental dissipation.

Fully depleting an electron layer on a time scale of the order of picoseconds, for most two-dimensional materials, is difficult. Thus, the protocol described above is, for currently available materials, challenging to carry out [79]. Is there a more practical way to release inseparable plasmons from this system? One possibility would be to modulate the electron density of one of the two layers at some frequency, and search for plasmons released at half that frequency [39]; this represents yet another realization of the dynamical Casimir effect. Beyond this, it is interesting to consider how such released plasmons could be detected along with their spectral distribution. One possibility is to search for far infrared narrow-band emission which results from their radiative decay. This technique has been used in early work on traditional semiconductor heterostructures [80–82] and more recently in graphene [83]. Moreover, the inseparability of $\pm \mathbf{q}$ plasmon

modes this system can release in a dynamical Casimir effect protocol should be detectable via correlations in fluctuations of the electric field on either side of the system, which in principle could be detected via near-field microscopy techniques [17–19]. Studies of these possibilities will be addressed in future work.

ACKNOWLEDGMENTS

[1] D. Pines and D. Bohm, A collective description of electron interactions: II. Collective vs Individual Particle Aspects of the Interactions, Phys. Rev. **85**, 338 (1952).

[2] D. Pines, Collective energy losses in solids, Rev. Mod. Phys. **28**, 184 (1956).

[3] K. Sawada, K. A. Brueckner, N. Fukuda, and R. Brout, Correlation energy of an electron gas at high density: Plasma oscillations, Phys. Rev. **108**, 507 (1957).

[4] G. Giuliani and G. Vignale, *Quantum Theory of the Electron Liquid* (Cambridge University Press, 2005).

[5] J. M. Pitarke, V. M. Silkin, E. V. Chulkov, and P. M. Echenique, Theory of surface plasmons and surface-plasmon polaritons, Rep. Prog. Phys. **70**, 1 (2007).

[6] R. H. Ritchie, Plasma losses by fast electrons in thin films, Phys. Rev. **106**, 874 (1957).

[7] T. Ando, A. B. Fowler, and F. Stern, Electronic properties of two-dimensional systems, Rev. Mod. Phys. **54**, 437 (1982).

[8] T. Stauber, Plasmonics in dirac systems: From graphene to topological insulators, J. Phys.: Condens. Matter **26**, 123201 (2014).

[9] T. Stauber, G. Gómez-Santos, and L. Brey, Spin-charge separation of plasmonic excitations in thin topological insulators, Phys. Rev. B **88**, 205427 (2013).

[10] T. Stauber, G. Gómez-Santos, and L. Brey, Plasmonics in topological insulators: Spin–charge separation, the influence of the inversion layer, and phonon–plasmon coupling, ACS Photonics **4**, 2978 (2017).

[11] A. Y. Nikitin, *Graphene Plasmonics*, World Scientific Handbook of Metamateriasl and Plasmonics, Vol. 1 (Word Scientific Publishing, 2017).

[12] A. Yu. Nikitin, F. Guinea, F. J. García-Vidal, and L. Martín-Moreno, Edge and waveguide terahertz surface plasmon modes in graphene microribbons, Phys. Rev. B **84**, 161407 (2011).

[13] F. H. L. Koppens, D. E. Chang, and F. J. García de Abajo, Graphene plasmonics: A platform for strong light–matter interactions, Nano Lett. **11**, 3370 (2011).

[14] T. M. Slipchenko, M. L. Nesterov, L. Martin-Moreno, and A. Yu. Nikitin, Analytical solution for the diffraction of an electromagnetic wave by a graphene grating, J. Opt. **15**, 114008 (2013).

[15] A. H. Castro Neto, F. Guinea, N. M. R. Peres, K. S. Novoselov, and A. K. Geim, The electronic properties of graphene, Rev. Mod. Phys. **81**, 109 (2009).

[16] M. I. Katsnelson, *Graphene* (Cambridge, 2012).

[17] J. Chen, M. Badioli, P. Alonso-González, S. Thongrattanasiri, F. Huth, J. Osmond, M. Spasenović, A. Centeno, A. Pesquera, P. Godignon, A. Zurutuza Elorza, N. Camara, F. J. G. de Abajo, R. Hillenbrand, and F. H. L. Koppens, Optical nano-imaging of gate-tunable graphene plasmons, Nature (London) **487**, 77 (2012).

[18] Z. Fei, A. S. Rodin, G. O. Andreev, W. Bao, A. S. McLeod, M. Wagner, L. M. Zhang, Z. Zhao, M. Thiemens, G. Dominguez, M. M. Fogler, A. H. C. Neto, C. N. Lau, F. Keilmann, and D. N. Basov, Gate-tuning of graphene plasmons revealed by infrared nano-imaging, Nature (London) **487**, 82 (2012).

[19] Z. Fei, A. S. Rodin, W. Gannett, S. Dai, W. Regan, M. Wagner, M. K. Liu, A. S. McLeod, G. Dominguez, M. Thiemens, A. H. Castro Neto, F. Keilmann, A. Zettl, R. Hillenbrand, M. M. Fogler, and D. N. Basov, Electronic and plasmonic phenomena at graphene grain boundaries, Nat. Nanotechnol. **8**, 821 (2013).

[20] L. Ju, B. Geng, J. Horng, C. Girit, M. Martin, Z. Hao, H. A. Bechtel, X. Liang, A. Zettl, Y. R. Shen, and F. Wang, Graphene plasmonics for tunable terahertz metamaterials, Nat. Nanotechnol. **6**, 630 (2011).

[21] F. Bonaccorso, Z. Sun, T. Hasan, and A. C. Ferrari, Graphene photonics and optoelectronics, Nat. Photonics **4**, 611 (2010).

[22] D. B. Farmer, D. Rodrigo, T. Low, and P. Avouris, Plasmon–plasmon hybridization and bandwidth enhancement in nanostructured graphene, Nano Lett. **15**, 2582 (2015).

[23] G. X. Ni, H. Wang, J. S. Wu, Z. Fei, M. D. Goldflam, F. Keilmann, B. Ozyilmaz, A. H. Castro Neto, X. M. Xie, M. M. Fogler, and D. N. Basov, Plasmons in graphene moire superlattices, Nat. Mater. **14**, 1217 (2015).

[24] P. Q. Liu, F. Valmorra, C. Maissen, and J. Faist, Electrically tunable graphene anti-dot array terahertz plasmonic crystals exhibiting multi-band resonances, Optica **2**, 135 (2015).

[25] D. Alcaraz Iranzo, S. Nanot, E. J. C. Dias, I. Epstein, C. Peng, D. K. Efetov, M. B. Lundeberg, R. Parret, J. Osmond, J.-Y. Hong, J. Kong, D. R. Englund, N. M. R. Peres, and F. H. L. Koppens, Probing the ultimate plasmon confinement limits with a van der waals heterostructure, Science **360**, 291 (2018).

[26] K. K. Gopalan, B. Paulillo, D. M. A. Mackenzie, D. Rodrigo, N. Bareza, P. R. Whelan, A. Shivayogimath, and V. Pruneri, Scalable and tunable periodic graphene nanohole arrays for mid-infrared plasmonics, Nano Lett. **18**, 5913 (2018).

[27] A. Yu. Nikitin, F. Guinea, F. J. Garcia-Vidal, and L. Martin-Moreno, Surface plasmon enhanced absorption and suppressed transmission in periodic arrays of graphene ribbons, Phys. Rev. B **85**, 081405 (2012).

[28] C. Vacacela Gomez, M. Pisarra, M. Gravina, J. M. Pitarke, and A. Sindona, Plasmon modes of graphene nanoribbons with periodic planar arrangements, Phys. Rev. Lett. **117**, 116801 (2016).

[29] N. M. R. Peres, A. Ferreira, Yu. V. Bludov, and M. I. Vasilevskiy, Light scattering by a medium with a spatially

modulated optical conductivity: The case of graphene, J. Phys.: Condens. Matter **24**, 245303 (2012).

[30] S. S. Sunku, G. X. Ni, B. Y. Jiang, H. Yoo, A. Sternbach, A. S. McLeod, T. Stauber, L. Xiong, T. Taniguchi, K. Watanabe, P. Kim, M. M. Fogler, and D. N. Basov, Photonic crystals for nano-light in Moirégraphene superlattices, Science **362**, 1153 (2018).

[31] L. Brey, T. Stauber, L. Martín-Moreno, and G. Gómez-Santos, Nonlocal quantum effects in plasmons of graphene superlattices, Phys. Rev. Lett. **124**, 257401 (2020).

[32] L. Brey, T. Stauber, T. Slipchenko, and L. Martín-Moreno, Plasmonic dirac cone in twisted bilayer graphene, Phys. Rev. Lett. **125**, 256804 (2020).

[33] T. Stauber, P. San-Jose, and L. Brey, Optical conductivity, drude weight and plasmons in twisted graphene bilayers, New J. Phys. **15**, 113050 (2013).

[34] C. F. G. Gilbert, A. Aspect, *Introduction to Quantum Optics* (Cambridge University Press, 2010).

[35] W. Vogel and D.-G. Welsch, *Quantum Optics* (Wiley, 2006).

[36] P. Törmä and W. L. Barnes, Strong coupling between surface plasmon polaritons and emitters: A review, Rep. Prog. Phys. **78**, 013901 (2015).

[37] C. Ciuti, G. Bastard, and I. Carusotto, Quantum vacuum properties of the intersubband cavity polariton field, Phys. Rev. B **72**, 115303 (2005).

[38] M. Berthel, S. Huant, and A. Drezet, Spatio-temporal second-order quantum correlations of surface plasmon polaritons, Opt. Lett. **41**, 37 (2016).

[39] Z. Sun, D. N. Basov, and M. M. Fogler, Graphene as a source of entangled plasmons, Phys. Rev. Res. **4**, 023208 (2022).

[40] D. E. Chang, A. S. Sørensen, P. R. Hemmer, and M. D. Lukin, Quantum optics with surface plasmons, Phys. Rev. Lett. **97**, 053002 (2006).

[41] A. González-Tudela, P. A. Huidobro, L. Martín-Moreno, C. Tejedor, and F. J. García-Vidal, Theory of strong coupling between quantum emitters and propagating surface plasmons, Phys. Rev. Lett. **110**, 126801 (2013).

[42] A. Gonzalez-Tudela, D. Martin-Cano, E. Moreno, L. Martin-Moreno, C. Tejedor, and F. J. Garcia-Vidal, Entanglement of two qubits mediated by one-dimensional plasmonic waveguides, Phys. Rev. Lett. **106**, 020501 (2011).

[43] L. A. Ponomarenko, A. K. Geim, A. A. Zhukov, R. Jalil, S. V. Morozov, K. S. Novoselov, I. V. Grigorieva, E. H. Hill, V. V. Cheianov, V. I. Fal'ko, K. Watanabe, T. Taniguchi, and R. V. Gorbachev, Tunable metal–insulator transition in double-layer graphene heterostructures, Nat. Phys. **7**, 958 (2011).

[44] T. Stauber and G. Gómez-Santos, Plasmons in layered structures including graphene, New J. Phys. **14**, 105018 (2012).

[45] D. Rodrigo, A. Tittl, O. Limaj, F. J. G. de Abajo, V. Pruneri, and H. Altug, Double-layer graphene for enhanced tunable infrared plasmonics, Light: Sci. Appl. **6**, e16277 (2017).

[46] S. Das Sarma and A. Madhukar, Collective modes of spatially separated, two-component, two-dimensional plasma in solids, Phys. Rev. B **23**, 805 (1981).

[47] L.-M. Duan, G. Giedke, J. I. Cirac, and P. Zoller, Inseparability criterion for continuous variable systems, Phys. Rev. Lett. **84**, 2722 (2000).

[48] S. L. Braunstein and A. K. Pati, *Quantum Information with Continuous Variables* (Kluwer Academic Publishers, 2003).

[49] V. V. Dodonov, Current status of the dynamical Casimir effect, Phys. Scr. **82**, 038105 (2010).

[50] P. D. Nation, J. R. Johansson, M. P. Blencowe, and F. Nori, Colloquium: Stimulating uncertainty: Amplifying the quantum vacuum with superconducting circuits, Rev. Mod. Phys. **84**, 1 (2012).

[51] M. Cirone, K. Rząz-dotewski, and J. Mostowski, Photon generation by time-dependent dielectric: A soluble model, Phys. Rev. A **55**, 62 (1997).

[52] N. Westerberg, A. Prain, D. Faccio, and P. Öhberg, Vacuum radiation and frequency-mixing in linear light-matter systems, J. Phys. Commun. **3**, 065012 (2019).

[53] A. V. Dodonov and V. V. Dodonov, Resonance generation of photons from vacuum in cavities due to strong periodical changes of conductivity in a thin semiconductor boundary layer, J. Opt. B: Quantum Semiclassical Opt. **7**, S47 (2005).

[54] J. Sloan, N. Rivera, J. D. Joannopoulos, and M. Soljačić, Casimir light in dispersive nanophotonics, Phys. Rev. Lett. **127**, 053603 (2021).

[55] J. Sloan, N. Rivera, J. D. Joannopoulos, and M. Soljačić, Controlling two-photon emission from superluminal and accelerating index perturbations, Nat. Phys. **18**, 67 (2022).

[56] B. Wunsch, T. Stauber, F. Sols, and F. Guinea, Dynamical polarization of graphene at finite doping, New J. Phys. **8**, 318 (2006).

[57] E. H. Hwang and S. Das Sarma, Dielectric function, screening, and plasmons in two-dimensional graphene, Phys. Rev. B **75**, 205418 (2007).

[58] L. Brey and H. A. Fertig, Elementary electronic excitations in graphene nanoribbons, Phys. Rev. B **75**, 125434 (2007).

[59] See Supplemental Material at http://link.aps.org/supplemental/10.1103/PhysRevB.109.045303 for more details with additional analytical results.

[60] J. M. Elson and R. H. Ritchie, Photon interactions at a rough metal surface, Phys. Rev. B **4**, 4129 (1971).

[61] T. Gruner and D. G. Welsch, Green-function approach to the radiation-field quantization for homogeneous and inhomogeneous Kramers-Kronig dielectrics, Phys. Rev. A **53**, 1818 (1996).

[62] A. Archambault, F. Marquier, J.-J. Greffet, and C. Arnold, Quantum theory of spontaneous and stimulated emission of surface plasmons, Phys. Rev. B **82**, 035411 (2010).

[63] G. W. Hanson, S. A. Hassani Gangaraj, C. Lee, D. G. Angelakis, and M. Tame, Quantum plasmonic excitation in graphene and loss-insensitive propagation, Phys. Rev. A **92**, 013828 (2015).

[64] B. A. Ferreira, B. Amorim, A. J. Chaves, and N. M. R. Peres, Quantization of graphene plasmons, Phys. Rev. A **101**, 033817 (2020).

[65] E. H. Hwang and S. Das Sarma, Plasmon modes of spatially separated double-layer graphene, Phys. Rev. B **80**, 205405 (2009).

[66] G. M. Alexey V. Kavokin, Jeremy J. Baumberg, and F. P. Laussy, *Microcavities* (Oxford University Press, 2007).

[67] A. Frisk Kockum, A. Miranowicz, S. De Liberato, S. Savasta, and F. Nori, Ultrastrong coupling between light and matter, Nat. Rev. Phys. **1**, 19 (2019).

[68] P. Kirton, M. M. Roses, J. Keeling, and E. G. Dalla Torre, Introduction to the Dicke model: From equilibrium to nonequilibrium, and vice versa, Adv. Quantum Technol. **2**, 1800043 (2019).

[69] J. J. Hopfield, Theory of the contribution of excitons to the complex dielectric constant of crystals, Phys. Rev. **112**, 1555 (1958).

[70] D. N. Makarov, Coupled harmonic oscillators and their quantum entanglement, Phys. Rev. E **97**, 042203 (2018).

[71] J.-Y. Zhou, Y.-H. Zhou, X.-L. Yin, J.-F. Huang, and J.-Q. Liao, Quantum entanglement maintained by virtual excitations in an ultrastrongly-coupled-oscillator system, Sci. Rep. **10**, 12557 (2020).

[72] S. M. Girvin and K. Yang, *Modern Condensed Matter Physics* (Cambridge University Press, Cambridge, 2019).

[73] Ulf Leonhardt, *Essential Quantum Optics* (Cambridge University Press, 2010).

[74] A. Woessner, M. B. Lundeberg, Y. Gao, A. Principi, P. Alonso-González, M. Carrega, K. Watanabe, T. Taniguchi, G. Vignale, M. Polini, J. Hone, R. Hillenbrand, and F. H. L. Koppens, Highly confined low-loss plasmons in graphene–boron nitride heterostructures, Nat. Mater. **14**, 421 (2015).

[75] M. B. Farias, C. D. Fosco, F. C. Lombardo, and F. D. Mazzitelli, Quantum friction between graphene sheets, Phys. Rev. D **95**, 065012 (2017).

[76] V. Despoja, P. M. Echenique, and M. Šunjić, Quantum friction between oscillating crystal slabs: Graphene mono-layers on dielectric substrates, Phys. Rev. B **98**, 125405 (2018).

[77] V. Dodonov, Fifty years of the dynamical Casimir effect, Physics **2**, 67 (2020).

[78] C. D. Fosco, F. C. Lombardo, and F. D. Mazzitelli, Motion-induced radiation due to an atom in the presence of a graphene plane, Universe **7**, 158 (2021).

[79] For example, for plasmons of sufficiently high frequency to be easily detected (bigger than 1THz), for ultrastrong coupling the electron density would have to vanish at roughly this rate or faster.

[80] D. C. Tsui, E. Gornik, and R. A. Logan, Far infrared emission from plasma oscillations of si inversion layers, Solid State Commun. **35**, 875 (1980).

[81] R. A. Höpfel, E. Vass, and E. Gornik, Thermal excitation of two-dimensional plasma oscillations, Phys. Rev. Lett. **49**, 1667 (1982).

[82] N. Okisu, Y. Sambe, and T. Kobayashi, Far-infrared emission from two-dimensional plasmons in AlGaAs/GaAs heterointer-faces, Appl. Phys. Lett. **48**, 776 (1986).

[83] Y. Li, P. Ferreyra, A. K. Swan, and R. Paiella, Current-driven terahertz light emission from graphene plasmonic oscillations, ACS Photonics, **6**, 2562 (2019).